Performance of Thermal Protection Systems in a Mach 7 Environment

Herman L. Bohon,* J. Wayne Sawyer,† L. Roane Hunt,† and Irving Weinstein†
NASA Langley Research Center, Hampton, Va.

The integrity and reusability of three flight-weight metallic and reusable surface insulation (RSI) thermal protection systems, designed for the space Shuttle entry environment, have been demonstrated. Each model successfully survived over 23 entry thermal cycles without serious degradation. The metallic systems were more tolerant of the hostile environment and provided a higher degree of reusability than did the RSI. Thermal expansion slip joints of the metallic TPS successfully prevented hot-gas ingress to the substructure. The RSI demonstrated high damage tolerance, and field repairs increased its reusability. Heat-transfer tests to further assess RSI gap heating indicate that stacked tile orientations may impose a penalty on tile thickness. Parameters influencing RSI impingement heating were determined and the heating data correlated.

Nomenclature

D	= tile length (Figs. 11 and 12), m
L	= gap length (Fig. 10), m
M_l	= local Mach number
Δ_p	= panel differential pressure, Pa
q	= heat-transfer rate, w/m^2
q_{fp}	= flat-plate heat-transfer rate, w/m^2
T	= temperature, K
s	= surface dimension on tile perimeter (Fig. 11), m
w	= gap width (Fig. 10), m
x	= surface dimension from midpoint of tile (Fig. 12), m
z	= depth below tile surface (Fig. 10), m
δ^*	= boundary-layer displacement thickness, m
θ	= slope of tile forward-facing wall (Fig. 10), deg

Introduction

THE Space Shuttle Orbiter design requirements call for a mission life of 100 entries into earth's atmosphere with minimal refurbishment between missions. State-of-the-art thermal protection systems (TPS) for current entry vehicles, however, are of the ablative type, capable of only single-entry survival. With the inception of the Space Shuttle and its multimission requirements, definition, and development of a fully reusable TPS was recognized as a major technology effort.[1-4] To resolve some of the technology voids, NASA Langley Research Center initiated a program to improve the state-of-the-art of TPS for application over a range of surface temperatures of 900-1600 K. Areas for technology advancement included the development of improved materials data base; cyclic creep predictions; local heating induced by joints, gaps, and seals; concept development; and performance demonstration of full-size systems.

In this paper the mission capability of three potential TPS candidates, including two radiative metallic and one reusable surface insulation (RSI) systems, is discussed. Large, full-size, flight-weight TPS panels were designed and fabricated, and subsequently subjected to repeated static thermal cycles and aerothermal tests in a Mach 7 stream to determine thermal efficiency and structural integrity of the basic concepts. The effects of surface irregularities and the performance of joints and seals in the presence of the hypersonic stream are reviewed. High local gap heating, observed on the RSI model and assessed by additional heat-transfer tests on simulated RSI tile arrays, is discussed and parameters affecting this heating are identified and the heating data correlated.

Presented as Paper 75-800 at the AIAA/ASME/SAE 16th Structures, Structural Dynamics, and Materials Conference, Denver, Colorado, May 27-29, 1975; submitted June 5, 1975; revision received July 18, 1975.

Index categories: Aircraft Testing (including Component Wind-Tunnel Testing); Radiation and Radiative Heat Transfer.

*Head, Thermal Protection Section, Structures and Dynamics Division. Member AIAA.

†Aerospace Engineer, Thermal Protection Section, Structures and Dynamics Division.

TPS Models

The TPS panels tested are shown in Fig. 1. All panels are 1.1 × 1.5 m in planform and are designed to accommodate the pressure and thermal loads of the Shuttle trajectory and prevent the substructure from exceeding 450 K maximum temperature limitation.

The Rene 41, nickel-base alloy panel is notable for its simplicity. The panel is designed for surface temperatures to 1100 K and has a single corrugated skin attached to the substructure by 5 rows of supports at 0.35 m spacing. The supports are designed to transmit a 21-kPa normal pressure load to the substructure. The 4 outer rows of supports provide virtually no resistance to longitudinal thermal growth. The center supports are rotated 90° from the outer supports (as shown in inset) to resist the surface drag loads. The insulation package is a foil-covered fibrous silica. Design details of this system are given in Ref. 5.

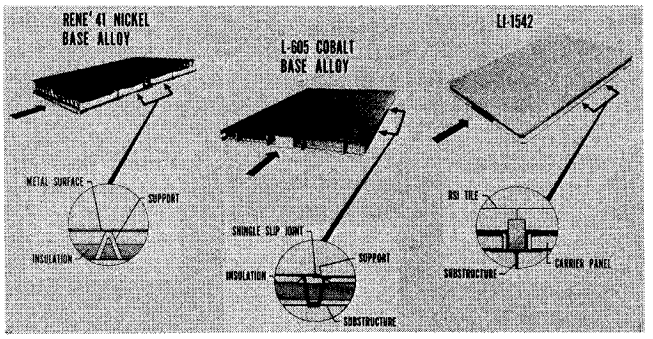

Fig. 1 Radiative thermal protection system (1.1 by 1.5m).

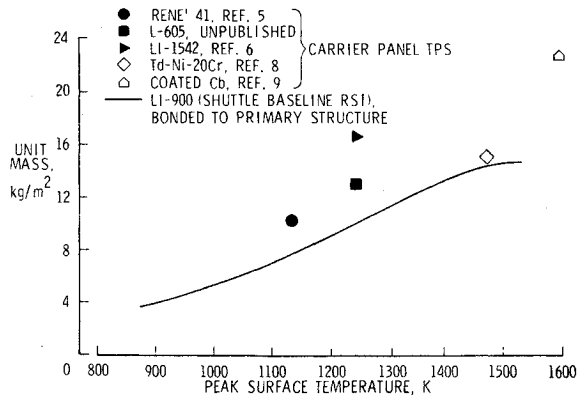

Fig. 2 Thermal protection system unit mass for Space Shuttle application.

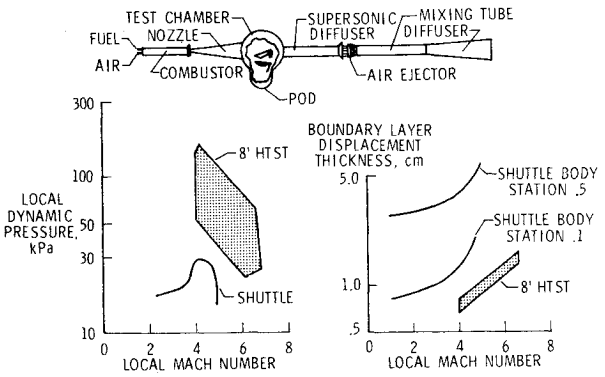

Fig. 3 Facility and test environment in Langley Research Center 8-ft HTST.

The L-605, cobalt-base alloy panel is corrugation-stiffened and is designed for application to a surface temperature of 1250 K. This panel has a riveted longitudinal splice and two transverse shingle-type slip joints (see inset), spaced 1 m apart, for thermal expansion. The supports are designed to minimize heat conduction to the substructure, yet have sufficient strength to withstand aerodynamic loads. The foil-covered fibrous silica insulation package is suspended from the corrugation.

The RSI panel consists of an array of coated silica tiles designated LI-1542.[6-7] While the RSI material will accommodate temperatures to 1530 K, the current tiles are 3-cm thick to withstand an entry heat pulse representative of a 1250-K surface temperature. The tiles have a thin borosilicate coating to impede water ingress and to resist erosion of the silica material due to aerodynamic shear. The eight center tiles are bonded to two stringer-stiffened carrier panels, which in turn attach to the substructure. Details of the thermal seal around each carrier panel are shown by the inset. All tiles are undercut as shown and a soft fibrous silica filler bar closes the void between the carrier panels. Each four-tile array is offset to break up flow in the longitudinal gaps.

The fabricated unit masses of these designs are shown in Fig. 2 by the solid symbols as a function of their respective peak surface design temperature. Also shown by the open symbols are the fabricated unit masses of a full-scale TD-Ni-Cr metallic panel[8] of a design similar to the L-605 system and a coated columbium panel.[9] The TD-Ni-Cr panel has successfully survived 100 simulated ascent and reentry thermal pressure cycles without excessive degradation. The solid curve shown for comparison is the unit mass of the Shuttle baseline RSI system, which consists of LI-900 tiles bonded directly to primary structure. With the exception of the LI—1542 TPS and the coated columbium panel, the unit masses of the other metallic TPS are seen to be comparable, but all are consistently higher than the Shuttle baseline RSI unit mass. However, as technology for metallic TPS improves, these masses are expected to decrease.

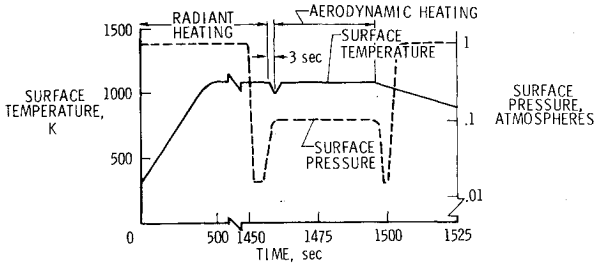

Fig.4 Typical aerothermal test cycle for Rene 41 panel.

Aerothermal Test Facility

The TPS were tested in the Langley 8-ft high-temperature structures tunnel (8-ft HTST) (Fig. 3), which is a large blowdown tunnel that simulates combinations of aerodynamic heating and pressure loading representative of flight at Mach 7 and altitudes between 25 km and 40 km. The high energy required for the simulation is obtained by burning a mixture of methane and air under pressure in the combustor and expanding the products of combustion through the test chamber.[10] TPS models are mounted in a large panel holder and retained in the pod area for protection during tunnel start and shutdown. The panel holder is a rectangular slab with a half-wedge leading edge. Boundary-layer trips and side fences assure uniform turbulent flow over the panel surface and pressure in a cavity behind the panel is controlled to produce a differential pressure loading during aerothermal tests.[10] Banks of radiant lamps, located in the pod, are used to preheat the panels through a prescribed portion of an entry thermal profile prior to rapid insertion into the Mach 7 stream. The lamps are also used to expose the panels to multiple-entry thermal cycles at 100 k Pa (1 atm) between wind-tunnel tests.

The range of test conditions and heating rates obtainable in the 8-ft HTST are available.[10] The plots at the bottom of Fig. 3 show the local dynamic pressure and boundary-layer displacement thickness over the surface of the panel as a function of local Mach number. Shown for comparison are corresponding values predicted for the bottom centerline of the Shuttle during entry. The local dynamic pressure is greater by a factor up to 5 than that of the Shuttle and the boundary layer in the tunnel is thinner; thus, surface-flow conditions over the test panel are more severe than the Shuttle entry flight conditions.

The procedure of conducting aerothermal tests in the 8-ft HTST is illustrated in Fig. 4. Panels are preheated with radiant lamps at 100 kPa (1 atm) to a prescribed point in the trajectory and then rapidly inserted into the Mach 7 stream for about 50 sec of aerothermal exposure at a freestream pressure of approximately 1 kPa (0.01 atm). During this period the local surface pressure, which is dependent on the panel holder angle of attack, provides the differential pressure loading. The temperature profile shown in Fig. 4 is also representative of that imposed on the panel during static thermal tests between wind-tunnel tests. Further details on test procedures are available.[11]

Performance of Full-Size TPS Panels

Metallic TPS

The Rene 41 panel was subject to a total of 37 complete thermal cycles at a surface temperature of 1140 K, including 11 insertions into the stream. Similarly, the L-605 panel was

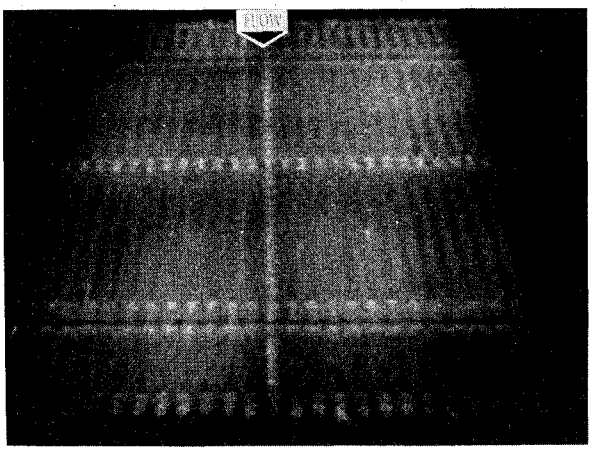

Fig. 5 Glowing L-605 TPS panel during aerothermal exposure.

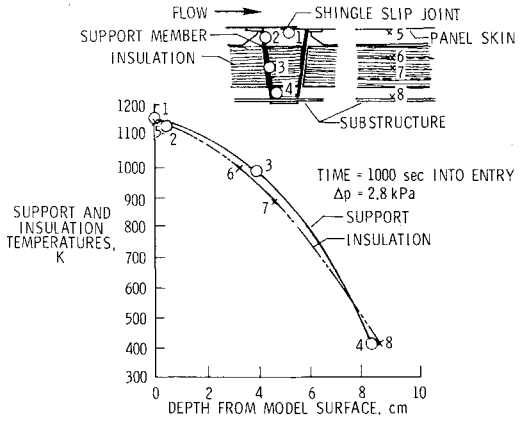

Fig. 6 Comparison of temperatures through shingle slip joint and insulation of L-605 panel.

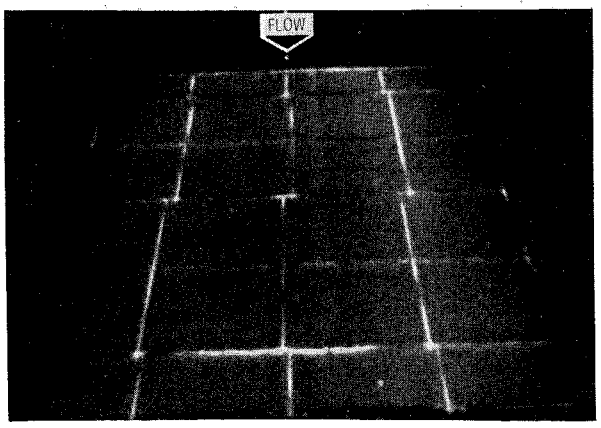

Fig. 7 Glowing LI-1542 TPS panel during aerothermal exposure.

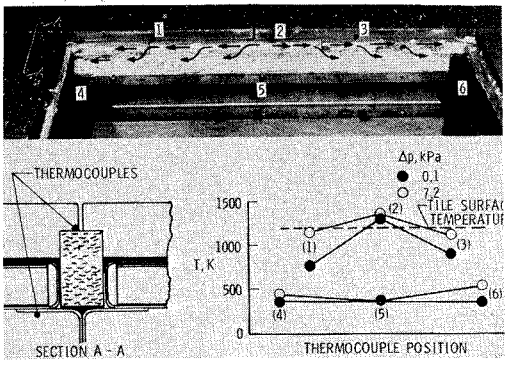

Fig. 8 Hot-gas penetration for LI-1542 TPS panel (after 40 sec of wind-tunnel exposure).

thermally cycled 32 times at a surface temperature of 1200 K with 13 wind-tunnel stream exposures. Both panels provided adequate thermal protection to the substructure throughout the test series.[5] A photograph of the L-605 panel in the windstream is shown in Fig. 5. The surface temperature is very uniform at about 1200 K. The bright glow is from round-head rivets, which attached the panel to the supports. This heating on protrusions is expected to be more pronounced in the thin boundary layer of the wind tunnel than that in actual flight.

The possibility of hot-gas ingress at slip joints has been an area of considerable concern with metallic TPS. However, the dark line or cool region at the transverse slip joint suggests that the simple shingle slip joints did prevent flow of hot gases to the interior. The performance of the slip joints is verified in Fig. 6 which shows the temperature distribution through the depth of the panel at a transverse joint and in the center of the panel. The temperatures are measured at 1000 sec into the simulated-entry profile, including 40 sec in the windstream. The differential pressure is 2.8 kPa inward. The temperature distribution along the supports at the slip joints shows no evidence of hot-gas ingress and, in fact, the heat conduction along the support is no more severe than that through the insulation. This is attributed to design features of the supports which prevent a direct heat path to the substructure.

The condition of the surface of the two metallic panels at the conclusion of the test series indicated the panels experienced no structural damage. Post-test vibration surveys and visual inspection of the disassembled models revealed no evidence of structural degradation of the supports or insulation system. Thus, the metallic TPS panels exhibited high integrity and good reusability in these tests.

LI-1542 RSI

Preliminary test results of the LI-1542 RSI panel are presented in Ref. 6. The panel was subjected to a total of 23 thermal cycles to 1200 K surface temperature with 12 wind-tunnel exposures. A photograph of the model in the Mach 7 stream is shown in Fig. 7. The top surface is at a uniform temperature of 1200 K; however, gap temperatures in some cases exceeded 1400 K. The bright spots at the offset in the longitudinal gaps indicate the high-pressure and high temperature region caused by flow in the gap impinging on the forward-facing wall of the downstream tile. The gaps around the carrier panels were observed to be at higher temperature than those interior to the carrier panels. (Recall that the eight center tiles are bonded to two carrier panels.) These higher temperatures are due in part to flow in the gaps and, in part, to inadequate thermal seals in the presence of an inward differential pressure. This phenomenon is evident in Fig. 8, which shows the results of hot-gas penetration to the substructure. In the photograph, the upstream carrier panel has been removed to expose the thermal seal and forward face of the downstream tile. The numbers on the figure indicate locations of the thermocouples in the gap and on the substructure. The thermocouple beads in the gap were positioned just under the lip of the recessed area, as indicated in the sketch. Note that thermocouple No. 2 is located where flow in the upstream longitudinal gap impinges on the downstream tile.

Thermocouple data are plotted in Fig. 8 (after 1100 sec of radiant heating and 40 sec in the windstream) for one test with $\Delta p = 0.1$ kPa (solid symbol) and for a test with $\Delta p = 7.2$ kPa (open symbols). The impingement temperature shown by thermocouple No. 2 exceeds the surface temperature shown by the dashed curve for both tests. In the $\Delta p = 0.1$ kPa test, temperatures at tile midpoints (thermocouple Nos. 1 and 3) were about the average of all other interior gap temperatures at

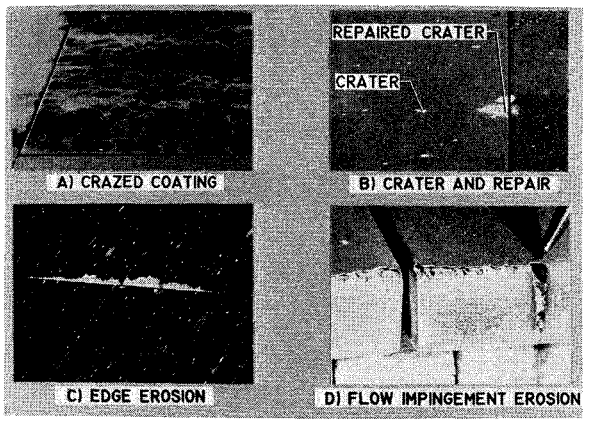

Fig. 9 Surface condition of LI-1542 panel after aerothermal exposure (23 thermal cycles, including 12 aerothermal tests). a) crazed coating; b) crater and repair; c) edge erosion; and d) flow impingement erosion.

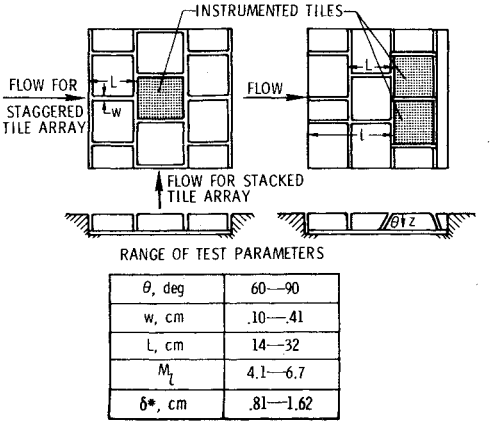

θ, deg	60—90
w, cm	.10—.41
L, cm	14—32
M_L	4.1—6.7
δ*, cm	.81—1.62

Fig. 10 Tile array and test parameters for gap heating test.

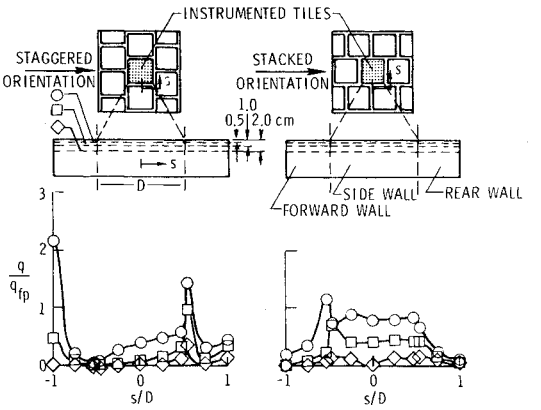

Fig. 11 Measured vertical wall heating to center tile ($w = 0.18$ cm; $\delta^* = 1.17$ cm).

that position and the substructure temperatures (thermocouple Nos. 4, 5, and 6) remained ambient. In the $\Delta p = 7.2$ kPa test, flow from the high-pressure region sought the path of least resistance and appeared to move laterally (as indicated by the flow arrows) toward the ends of the seal which formed a poor joint with the longitudinal seal and, thus, flow penetrated to the substructure. As a result, gap temperatures of the midpoint locations increased to about the average surface temperature and the substructure temperature increased as much as 280 K during the 40 sec of wind-tunnel exposure. The lack of temperature increase at thermocouple No. 5 indicates gas flow did not penetrate directly through the seal.

The LI-1542 model showed no evidence of structural degradation during the test series. However, the RSI tiles suffered considerable damage. Typical damage of the RSI surface is shown in Fig. 9. The borosilicate coating became crazed, as shown in Fig.9a early in the series. Although the cracks are not visible to the naked eye, the coating will not prevent water ingress. Nevertheless, no spalling or flaking of the coating occurred, probably because thermal stresses in the RSI are very low when the coating is crazed.

The tiles also had considerable damage in the form of craters caused by small foreign particles in the stream (Fig. 9b). The larger craters were successfully field repaired with a high-density borosilicate material (unfired coating) without further degradation. Another type of damage was erosion of the RSI at a forward-facing step (Fig.9c) and in the flow impingement region (Fig. 9d). The step was only about 6% of the boundary-layer displacement thickness, but was a source for high heating until the edge eroded to the height of the tile ahead of it. All flow impingement areas showed evidence of high heating and some tiles had been eroded as much as 1 cm into the face of the tile at the conclusion of the test series (Fig. 9d). Post-test inspection indicated that the penetrations had been caused by particle impact, high shear erosion, and, in some cases, small amounts of melting of the silica. All of the erosion which occurred probably was more pronounced in these wind-tunnel tests than it would be in actual flight since the boundary layer is thinner (Fig. 3) and the shear force is larger. Although the RSI tile surface would not meet the Shuttle requirement for reuse at the conclusion of the tests, the tiles demonstrated a high degree of damage tolerance without castastrophic failure.

RSI Impingement Heating

The potential impact of impingement heating observed on the LI-1542 model is uncertain because of the dearth of data available to delineate the variables affecting the heating rates. Although the baseline tile orientation for the Shuttle Orbiter is a stacked array of tiles, wherin the longitudinal gaps are aligned but skewed to the flow, the logistics of tile installation would be greatly simplified if a random or staggered tile array were permissible. To assess the problems of using a staggered tile array, a series of heat-transfer tests was conducted in the Langley Research Center 8-ft HTST to identify the parameters influencing impingement heating and to define limitations to staggered tile orientation.[12]

The models used for this study (Fig. 10) were arrays of tiles, nominally 0.15×0.15 m, with the heat transfer measured to a thin-wall metallic tile located near the center of the array. One model (see sketch at top left of Fig. 10) was arranged symmetrically so that both staggered and stacked tile orientations could be tested; the other model was arranged to study the effects of length and width of longitudinal gaps and slope of the forward-facing wall on the heating rate in a staggered tile orientation. The range of test parameters is listed at the bottom of Fig. 10.

The influence of tile orientation on gap heating is shown in Fig. 11, where cold-wall heating rates along the vertical walls of the tile are shown for staggered and stacked arrays. The vertical walls of the instrumented tile are shown unfolded above the measured data to permit easy correlation of heating data with position on the tile. Heating rates are nondimesionalized by the flat-plate value obtained from the top surface of the tile. These values were consistent with measured values on a flat calibration plate.[12] Data are shown for three locations near the top of the sidewall, beginning at the middle of the upstream wall ($s/D = -1$) and proceeding around the tile to the middle of the downstream wall ($s/D = +1$). Thermocouples are located at each of the symbol points on the data plots.

The heating rates measured on the staggered orientation in the impingement region were greater than twice the flat-plate

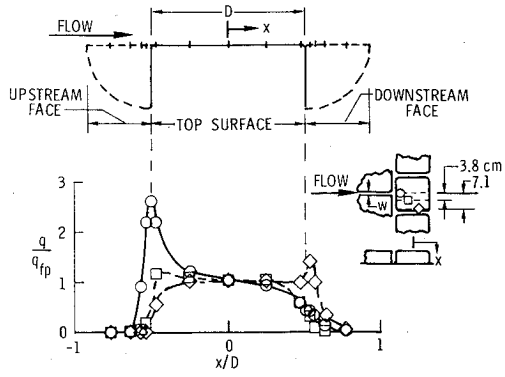

Fig. 12 Longitudinal heating distributions on center tile in staggered array ($w = 0.18$ cm; $\delta^* = 1.17$ cm).

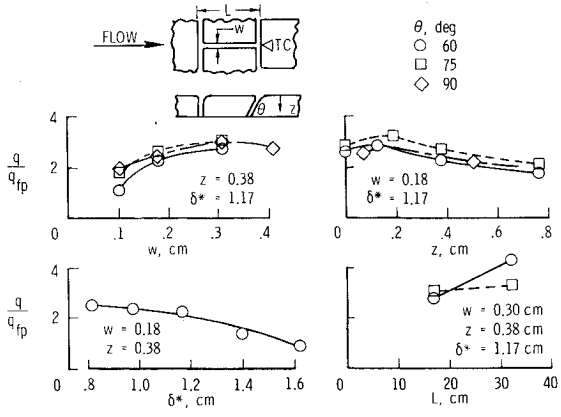

Fig. 13 Effect of test parameters on gap impingement heating to tile array.

value at the top of the wall, but dissipated rapidly a small distance from that point. A second less severe spike occurred at the downstream corner, which was influenced by flow in the longitudinal gap stagnating at the impingement region on the next tile. In the stacked orientation, there appears to be no significant spikes or hot spots; however, the entire length of the streamwise wall has a higher heating rate than the same wall in the staggered array. For the staggered array, the development of flow in the longitudinal gap can occur over only one tile length, whereas, for the stacked array, the longitudinal gap is continuous.

Integration of the heating rates revealed that the total heat load to the vertical walls of the stacked array is about 40% greater than the heat load to the vertical walls of the staggered array. This could impose a penalty on tile thickness for the stacked orientation and consequently, staggered tile orientation may be preferred over stacked orientation, but only if impingement heating is tolerable.

A typical longitudinal heating-rate distribution on the staggered tile array is shown on Fig. 12. Curves faired through the data are shown for three locations along the tile, as indicated on the inset. Tick marks on the model profile at the top of the figure indicate thermocouple locations. The highest heating rate registered was from the thermocouple on the upstream corner radius in the impingement region.

Impingement heating trends are shown in Fig. 13 as a function of each test parameter studied. As noted in the figure, in some cases impingement heating rates are as much as three times the local flat-plate value. The heating-rate ratio shows nonlinear variations as a function of width of the longitudinal gap w and boundary-layer displacement thickness δ^*. The cold-wall heating rate increases with increasing gap width and decreases with increasing boundary-layer displacement thickness. The variation in cold-wall heating rates appears as a linear function of the distance z for small distances from the

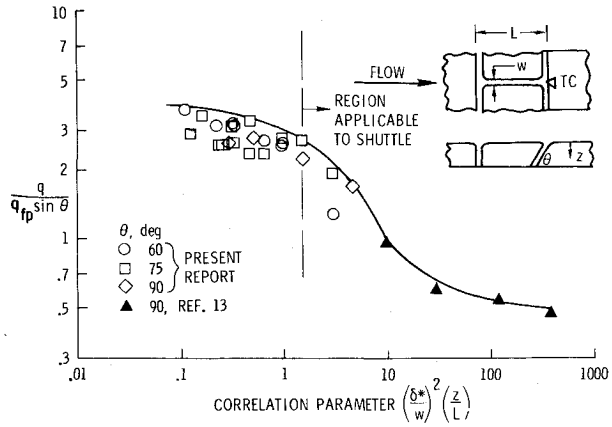

Fig. 14 Correlation of gap impingement heating.

top surface. The influence of gap length L is shown is Fig. 13 for the 60° sloping tile in the 32-cm gap length configuration.) The tread for the 60° sloping tile suggests a strong influence of gap length; however, the 75° sloping tile at the end of the 32-cm gap registered a lower heating-rate ratio than did the 60° tile. Post-test inspection indicated a lateral misalignment of thermocouples at the end of the 32-cm gap registered a lower heating-rate ratio than did the 60° tile. Post-test inspection indicated a lateral misalignment of thermocouples at the end of the 32-cm tap on the 75° sloping tile, and temperature response in the impingement region is found to be very sensitive to lateral position. Future tests will be directed toward identifying the zone of impingement heating. The effect on impingement heating of sloping the forward-facing wall is not clear. The heating-rate data show an increase between 60° and 75° sloping tiles, but the results for 90° but the results for 90° tiles were not consistent with this trend.

The impingement heating data from all tests have been correlated in a manner similar to that presented in Ref. 13 which suggests a correlation parameter consisting of the product of the test variables. The resulting parameter which provides a good correlation of the data is as follows

$$q/q_{fp}\sin\theta = g[(\delta^*/w)^2 z/L]$$

and the data are shown correlated in Fig. 14. The open symbols shown on the figure are the data obtained in the present investigation in a thin turbulent boundary layer with displacement thicknesses ranging from 0.81 to 1.62 cm. The solid symbols are for data obtained in a thick turbulent boundary layer with a displacement thickness of 12 cm.[13,14] The solid line is a faired curve approximating the upper bound of all the impingement heating data.

The region of the impingement heating curve applicable to the Shuttle, identified in Fig. 14, is based on current baseline design values of the tile geometry and calculated values of displacement thickness. Of course, the most critical region from the standpoint of tile temperature is the lowest value of the correlation parameter which occurs in flight when the boundary layer is thinnest in combination with high surface temperatures. These conditions would occur along the bottom centerline of the Orbiter vehicle and toward the end of the peak heating phase of the Shuttle entry. Preliminary calculations indicate that, at a body station of 0.1, tiles in a staggered orientation may reach temperatures above the design temperature at the impingement point. However, for most of the vehicle surface area, including the bottom surface, staggered orientation of the RSI tile appears to be feasible.

Conclusions

Large flight-weight radiative metallic and RSI thermal-protection systems were subjected to multiple static thermal

and aerothermal tests to assess their integrity and reusability in an enviroment simulating re-entry into the earth's atmosphere. The fabricated unit mass of the metallic systems were shown to be comparable to, but higher than, the unit mass of the Shuttle LI-900 RSI bonded to primary structure. All of the models successfully survived the test series without serious degradation; however, the metallic systems demonstrated a higher degree of reusability than did the RSI. Simple shingle-type slip joints used with the metallic TPS were sufficient to prevent hot-gas ingress to the substructure.

The RSI panel demonstrated high damage tolerance, even after surface degradations consisting of cracks, eroded edges, and craters. Successful field repairs to the RSI surface increased its reusability. Several problems associated with RSI gaps were identified. Pressure gradients may induce transverse flow in gaps which can significantly increase gap heating. Stacked tile orientation is susceptible to flow in gaps causing increased sidewall heating which could impose a tile thickness penalty. Staggered tile orientations are subject to local impingement heating rates as much as three times the flat-plate value; however, parameters influencing impingement heating have been identified and the heating data correlated. Based on these data, it appears that use of a randomly staggered tile orientation, which could facilitate installation of tiles, may be feasible over most of the surface of the Shuttle Orbiter.

References

[1] Anderson, R.A., Brooks, W.A., Jr., Leonard, R.W., and Malz, J., "Structures—A Technology Overview," *Astronautics and Aeronautics*, Vol. 9. Feb. 1971, pp. 38-47.

[2] Love, E.S., "Advanced Technology and Space Shuttle," *Astronautics & Aeronautics*, Vol. 2, Feb. 1973, pp. 30-66.

[3] Stein, B. A., Bohon, H.L., and Rummler, D.R., "An Assessment of Radiative Metallic Thermal Protection Systems for Space Shuttle," NASA TM X-2570, July 1972.

[4] Greenshields, D.H., Meyer, A.J., and Tillian, D.J., "Status of RSI TPS Technology Programs," NASA TM X-2570, July 1972.

[5] Deveikis, W.D., Miserentino, R., Weinstein, I., and Shideler, J. L., "Aerothermal Performance and Structural Integrity of a Rene 41 Thermal Protection System in a Mach 6.6 Stream," NASA TN D-7943, Nov. 1975.

[6] Hunt, L.R. and Bohon, H.L., "Performance of LI-1542 Reusable Surface Insulation System in a Hypersonic Stream" NASA , TM X-71955, April 1974.

[7] Burns, A.B., "Structural Evaluation of Candidate Space Shuttle Thermal Protection Systems," NASA, CR-132428, June 1972.

[8] Eidenoff, H.L. and Rose, L., "Thermal-Structural Evaluation of TD Ni-20 Cr Thermal Protection System Panels," NASA, CR-132487, June 1974.

[9] Rummler, D.R. and Black, W.E., "Evaluation of Coated Columbium for Thermal Protection Systems Application," AIAA Paper 75-817, 1975, Denver, Colo.

[10] Deveikis, W.D. and Hunt, L.R., "Loading and Heating of a Large Flat Plate at Mach 7 in the Langley 8-ft High-Temperature Structures Tunnel," NASA, TN D-7275, Sept. 1973.

[11] Deveikis, W.D., Bruce, W.E., Jr., and Karns, J.R., "Techniques for Aerothermal Tests of Large, Flightweight Thermal Protection Panels in a Mach 7 Wind Tunnel," NASA, TM X-71983, July 1974.

[12] Weinstein, I., Avery, D.E., and Chapman, A.J., "Aerodynamic Gap Heating on a Simulated RSI Tile Array in Turbulent Flow," NASA, TM X-3225, Nov. 1975.

[13] Dunavant, J.C. and Throckmorton, D.A., "Aerodynamic Heat Transfer to RSI Tile Surfaces and Gap Intersections," *Journal of Spacecraft and Rockets*, Vol. 11, June 1974, pp. 437-440.

[14] Throckmorton, D.A., "Heat Transfer to Surface and Gaps of RSI Tile Arrays in Turbulent Flow at Mach 10.3," NASA, TM X-71945, April 1974.